Flux Pinning in NbTi/Nb Multilayers

J. D. McCambridge, N. D. Rizzo*, X. S. Ling†, J. Q. Wang, and D. E. Prober
Department of Applied Physics, Yale University, New Haven, CT 06520-8284

L. R. Motowidlo and B. A. Zeitlin
IGC Advanced Superconductors Inc., Waterbury, CT 06704

Abstract—We made thin film multilayers of NbTi and Nb ($d_{NbTi} \approx$ 20 nm and $d_{Nb} \approx$ 3-9 nm). Samples were characterized by electrical transport measurements between 4.2 K and T_c, in magnetic fields up to 6 T. We present J_c as a function of the device geometry and orientation of the field. For some multilayers, J_c had a large peak whose onset occurs near ~ 0.2 H_{c2}. We suggest this peak effect is caused by a softening of the tilt modulus. Measured critical current densities at 4.2 K of 16 kA/mm^2 at 3 T and 8 kA/mm^2 at 5 T are among the highest achieved in the NbTi system.

INTRODUCTION

There has been renewed interest in the properties of layered metallic superconductors in recent years, both in their upper critical field [1]-[4] and critical current behavior [5], [6], mostly because of their analogous structure to high T_c compounds. Our work focuses on understanding (and improving) flux pinning in NbTi wires--especially wire using artificial pinning centers (APCs) [7], [8]. (Randomly positioned pinning centers are obtained by the precipitation heat treatments of conventional processing [9].) APC techniques have the advantage of being able to change pinner geometry and material. We made and measured NbTi/Nb multilayers with geometries comparable to those of APC wires in order to better understand the behavior of the technologically important properties of such multicomponent superconductors: T_c, H_{c2}, and particularly, J_c. For APC wires with Nb pinner, it is found that the optimum pin size and spacing are on the order of the coherence length ($\xi \approx$ 5 nm) and vortex lattice spacing ($a \approx$ 22 nm at 5 T) respectively [7].

SAMPLE FABRICATION AND MEASUREMENT

We sputter deposited single films and multilayers of Nb and Nb-47 wt.% Ti ($Nb_{0.37}Ti_{0.63}$) onto radiatively-heated, oxidized Si wafers (typically ~ 0.25 mm thick with a 200 nm SiO_2 layer). Deposition temperature was ~ 250 °C. The Nb target was 99.995% pure, while the NbTi target was 99.99% pure. The NbTi was RF sputtered (because of target surface oxidation) at a power density of 15 W/cm^2 . We found it necessary to use a Cu-backed NbTi target to prevent overheating, which caused the deposition rate to drift. The Nb was DC sputtered at 5 W/cm^2. The background pressure of the chamber during deposition was less than ~ 0.7 mPa; 1.33 Pa Ar was used as the sputtering gas. With these conditions, the Nb deposition rate was ~ 0.15 nm/s and the NbTi rate was ~ 0.25 nm/s.

The single component films were typically 200 nm thick. Each multilayer had a ~ 50 nm buffer layer of Nb, followed by 10 periods of alternating NbTi and Nb, and finished with a ~ 50 nm cap layer of Nb. The deposition rates were measured (by profilometer) before each run and the shutter times appropriately adjusted. Four multilayers were fabricated: the NbTi thickness d_{NbTi} was held at ≈ 20 nm, while the Nb thicknesses were $d_{Nb} \approx$ 3, 5, 7, and 9 nm (see Table 1). Attempts to independently confirm the multilayer geometry by small angle x-ray diffraction were unsucessful due to the long periods (Λ = 23-30 nm) and the thick cap layers of the samples. The buffer and cap layers served to prevent possible interdiffusion with the substrate and surface oxidation, and to reduce the effects of surface superconductivity [3].

We used standard liftoff photolithography (AZ 5218) to pattern a sputter-deposited layer of ~ 200 nm Al, which served as the etch mask and contact metal. The samples were then reactive ion etched (RIE) in SF_6 to produce 3 μm wide by 60 μm long (between the voltage taps) wires in a standard four probe configuration. Two sets of RIE conditions were used: 30 Pa, 30 sccm, ~ 0.5 W/cm^2 and 0.5 Pa, 10 sccm, ~ 2.5 W/cm^2. Both etch rates were comparable (~1 nm/s), however, the latter conditions were preferred for their minimal undercut (higher anisotropy). The SiO_2 served as an etch stop layer. In some later samples it was omitted. The contact pads were protected with photoresist and the Al was then removed in the device area using either a solution of 20 wt.% NaOH or commercial Al etch (PAE), neither of which attacks Nb or NbTi. PAE was preferred for its slower etch rate and because it does not attack photoresist. Samples without a contact layer had high contact resistances and hence heating problems at high current densities. Some samples were made without removing the Al layer over the wire--they occasionally had parasitic shunt resistances which prevented accurate electrical measurements. After patterning, each sample was examined in a scanning electron microscope to confirm its dimensions.

Table 1. Multilayer Properties

SAMPLE	d_{NbTi} (nm)	d_{Nb} (nm)	Tc (K)
NbTi	200	n/a	8.98
A (20/3)	19.9	2.9	9.03
B (20/5)	20.4	4.8	9.02
C (20/7)	20.5	6.6	9.22
D (20/9)	20.2	9.2	9.68
Nb	n/a	200	9.79

Manuscript received October 16, 1994.
This work was supported by CT Dept. Econ. Dev. grant No. 92G036, NSF contract No. III-9203072, and IGC.
*Department of Physics, Yale University
†Present address NEC Research Institute, Inc., Princeton, NJ 08540

1051-8223/95$04.00 © 1995 IEEE

We made two types of transport measurements at a variety of temperatures, magnetic fields, and field orientations to the layers. We measured the DC current-voltage characteristics (I-Vs) using a battery with a series resistor to supply current and a Keithley 147 Nanovolt Null Detector to measure the voltage. Some later measurements used a Yokogawa 7651 Power Supply as the current source--no differences were detected between the two methods. I_c was defined by a voltage criterion of 0.33 μV. We found the upper critical field $H_{c2}(T)$ of each sample by measuring the AC sample resistance (with a PAR 124 lock-in amplifier) versus temperature at fixed fields. The excitation current was 1 μA. $T_c(B)$ was defined at $R_n/2$. The variable-temperature cryostat has a rotating stage which enabled us to vary the angle θ between the sample surface and the applied field (see Fig. 1). The transport current was always perpendicular to the field. We were unable to rotate the samples *in situ*, so θ was fixed at 5° or 90° relative to the cryostat axis (which was collinear with the field, ± 0.5°) for the measurements in this paper. We estimate the total uncertainty in θ was no more than 1.5°. Since $H_{c2}(\theta)$ and $J_c(\theta)$ have cusps at 0° [4]-[6], we moved intentionally away from true parallel to reduce systematic errors due to possible misalignment.

RESULTS AND DISCUSSION

In Table 1 we present the zero-field critical temperatures versus d_{Nb}. As the thickness of the Nb layer increases, the T_c of the multilayer approaches that of our thick Nb film. Conversely, as d_{Nb} decreases, the T_c approaches that of our thick NbTi film. Earlier work by Obi *et al.* [1] found an unusual dip in the critical temperatures (below the T_c of either constituent) of somewhat similar NbTi/Nb multilayers, which they tentatively attributed to localization effects. However, the behavior in Table 1 is that expected for a multilayer composed of two superconductors [10].

We plot the upper critical fields $H_{c2}(T)$ at θ = 5° for a NbTi film and two representative NbTi/Nb multilayers in Fig. 1. Sample D (and sample C, not shown) has the expected 3D to 2D crossover of the superconducting order parameter Δ(r) at T^* [1]-[6], [11]. Sample B shows some indication of dimensional crossover as well. Where ξ is large (near T_c), Δ(r) extends over many layers, yielding averaged 3D behavior. As ξ decreases, Δ(r) can be concentrated in the cleaner layer (Nb in our case), yielding quasi-2D behavior. The multilayers and films are only mildly anisotropic--near T_c, the ratio of the near parallel (θ = 5°) to perpendicular upper critical field slopes is < 1.2 for all samples studied. There is significant proximity-effect enhancement of $H_{c2}(T)$ compared to our NbTi film at low fields for d_{Nb} > 5 nm. Above ~ 5 T, all multilayers suffered from proximity-effect depression of $H_{c2}(T)$.

The most striking results are plotted in figure 2. We compare the critical current density versus field at θ = 5° of a 200 nm NbTi film to the $J_c(5°)$ of two multilayers: samples A (20/3) and B (20/5). Jc of the NbTi film is not large, showing that the pinning is fairly weak as expected for NbTi with no precipitation heat treatments; J_c decreases monotonically with B. The same is true of sample A. However, sample B

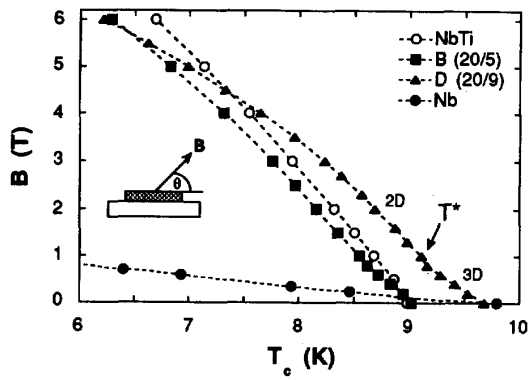

Fig. 1. Upper critical fields $H_{c2}(T)$ at θ = 5°.

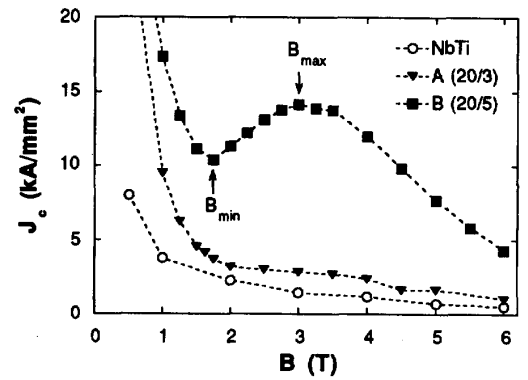

Fig. 2. Critical current density J_c vs. applied field B at θ = 5° and 4.2 K

shows a pronounced peak in J_c and much stronger pinning overall. The critical current densities of our multilayers are much higher than that of bulk NbTi, even optimized conventional wire [9]. This peak effect is seen in samples C and D, as well as layered superconductors made by other groups [5], [6], [12]. Our values of J_c are larger than those observed by those workers. We believe the large peak of J_c we observe is a "bulk" effect and is not due to the limited thickness of our samples. Thin films (d < λ) can have J_c larger than the bulk [13]. However, we only find such large J_c in the layered samples.

In Fig. 3 we plot $J_c(B)$ at θ = 5° for sample D at 4.2, 6.0, and 7.0 K. $J_c(B)$ for sample B at 4.2 K is provided for comparison. The magnitude of the peak decreases and its onset in field (marked in Figs. 2 and 3 as B_{min}) shifts downward as the temperature increases [5], [6]. B_{min} also shifts downward in field as d_{Nb} is increased [5]. We also find that $J_c \sim 1/\sin\theta$ at fixed field and B_{min} shifts outward as θ increases, similar to Koorevaar *et al.* [5]. In the inset of Fig. 3 we plot the global pinning force density $F_p = J_cB$ as a function of field for samples B and D at 4.2 K. There is a

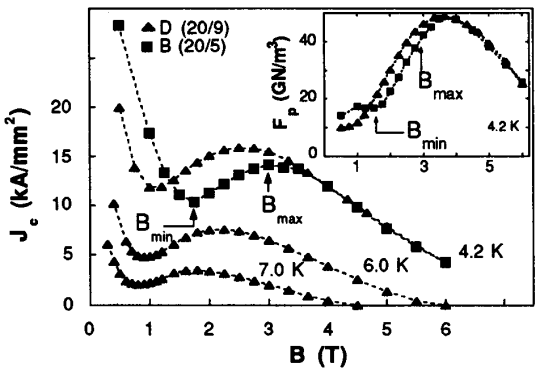

Fig. 3. Temperature dependence of the critical current density J_c vs. applied field B at $\theta = 5°$. Inset: global pinning force density F_p vs. field B at 4.2 K.

clear change in the pinning behavior at B_{min}, but no corresponding change at B_{max}, the field of peak J_c.

The explanation for the peak effect in layered superconductors is usually given in terms of a crossover from "isotropic" vortex motion to anisotropic motion: at low fields, the vortex lattice can be appropriately described as an anisotropic Abrikosov lattice [5], but at higher fields, the vortices become kinked, and can be described in the step-wise vortex model of Takahashi and Tachiki [14]. The kinked vortex lattice is more strongly pinned than the unkinked lattice and this produces a peak in J_c near the crossover. But what drives this crossover and where does it occur in field (and temperature)?

Nojima *et al.* [6] have suggested that a possible mechanism is the transition from proximity-coupled Nb layers (through the Nb-alloy) to decoupled Nb layers, which they claim occurs at B_{max} (see Figs. 2 and 3). However, Koorevaar *et al.* [5] found little or no dependence of B_{max} on the Nb-alloy thickness. In turn, Koorevaar *et al.* propose that the formation energy of a kink (versus straight) could be a barrier to flux-line motion, and that the kink is fully formed at B_{max}. We suggest a different explanation: softening of the tilt modulus c_{44} in a layered system, with B near parallel to the planes, is the mechanism which drives the smooth crossover from weak to strong pinning and that it occurs at B_{min}.

Larkin and Ovchinnikov suggested that a peak effect may arise from the onset of plastic distortion of the vortex lattice in the case of sparse, strong pinners [15]. This onset occurs when the elementary pinning force of a defect exceeds the "rigidity" of the vortex lattice: $f_p > a^2(c_{66}c_{44})^{1/2}$, where a is the vortex lattice spacing and c_{66} is the shear modulus [16]. We believe that plastic distortion of the vortex lattice in our layered samples is the cause of the peak in J_c.

For a layered superconductor, we neglect the weak, random pinning of the NbTi grain boundaries and consider only the intrinsic pinning due to the layering. (The NbTi film indeed has much weaker pinning, see Fig. 2.) Recently, it has been shown that the interface between two superconductors with dissimilar penetration depths can have a high elementary pinning force f_p [17]. Since this intrinsic pinning has a well-defined wavelength $\Lambda = d_{NbTi} + d_{Nb}$, it seems reasonable to consider distortions of the vortex lattice with Fourier components related to Λ^{-1}. The shear modulus c_{66} is not dispersive, but c_{44} depends strongly on the wavevector of the distortion $\mathbf{k}$ and the penetration depth λ [18], [19]. The temperature and structural dependence of the peak effect may therefore be due to the softening of c_{44}, and thus of the rigidity of the vortex lattice, relative to the intrinsic pinning force f_p. Our calculations are in an early stage, since the behavior of f_p is not well known; we estimate $f_p \sim a^2(c_{66}c_{44})^{1/2} \sim 10^{-11}$ N at low fields and intermediate temperatures.

CONCLUSION

We produced NbTi/Nb multilayers as a model system for investigating flux pinning in artificial pinning center (APC) wires. The critical current densities achieved in our layered structures are *very* large (17 kA/mm^2 at 3 T, 8 kA/mm^2 at 5 T) and we observed a peak effect for some of the multilayers. We suggest the peak effect is caused by a softening of the tilt modulus c_{44} relative to the periodic intrinsic pinning of the layers.

ACKNOWLEDGMENTS

We thank M. J. Rooks of the National Nanofabrication Facility at Cornell University for making the photolithography masks. Our thanks to P. Chalsani and S. B. Weiss for technical assistance.

REFERENCES

[1] Y. Obi, M. Ikebe, Y. Muto, and H. Fujimori, "Upper critical fields of NbTi based multilayered materials," Jap. J. Appl. Phys., vol. 26-3, pp. 1445-1446, 1987.
[2] M. G. Karkut *et al.*, "Anomalous upper critical fields of superconducting multilayers: verification of the Takahashi-Tachiki effect," Phys. Rev. Lett., vol. 60, pp. 1751-1754, 1988.
[3] J. Aarts, K.-J. de Korver, and P. H. Kes, "Dimensionality crossovers in the parallel critical fields of $Nb/Nb_{0.6}Zr_{0.4}$ multilayers," Europhys. Lett., vol. 12, pp. 447-452, 1990.
[4] Y. Kuwasawa, U. Hayano, T. Tosaka, S. Nakano, and S. Matuda, "Observation of anomalous transition in the upper critical fields of $Nb/Nb_{0.5}Zr_{0.5}$ multilayers," Physica C, vol. 165, pp. 173-178, 1990.
[5] P. Koorevaar, W. Maj, P. H. Kes, and J. Aarts, "Vortex-lattice transition in superconducting NbZr/Nb multilayers," Phys. Rev. B, vol. 47, pp. 934-943, 1993.
[6] T. Nojima, M. Kinoshita, S. Nakano, and Y. Kuwasawa, "Transport critical current density and dimensional crossover in superconducting NbZr/Nb multilayers," Physica C, vol. 206, pp. 387-392, 1993.
[7] L. R. Motowidlo, B. A. Zeitlin, M. S. Walker, and P. Haldar, "Multifilament NbTi with artificial pinning centers: the effect of alloy and pin material on the superconducting properties," Appl. Phys. Lett., vol. 61, pp. 991-993, 1992.
[8] K. Matsumoto *et al.*, "Flux pinning characteristics of Nb artificial pins with ribbon-shape in Nb-46.5 wt% Ti superconductors," Supercond. Sci. Tech., vol. 5, pp. 684-689, 1992.
[9] C. Meingast, P. J. Lee, and D. C. Larbalestier, "Quantitative description of a high J_c NbTi superconductor during its final optimization strain: I. Microstructure, T_c, H_{c2}, and resistivity," J. Appl. Phys., vol. 66, pp. 5962-5970, 1989.
[10] J. H. Chen, "Proximity effect in zero field with the Landau-Ginzburg equation. II," Phys. Rev. B, vol. 42, pp. 3957-3959, 1990, and references therein.
[11] S. Takahashi and M. Tachiki, "Theory of the upper critical field of superconducting superlattices," Phys. Rev. B, vol. 33, pp. 4620-4631, 1986; S. Takahashi and M. Tachiki, "New phase diagram in superconducting superlattices," *ibid.*, vol. 34, pp. 3162-3164, 1986.

[12] H. Raffy, J. C. Renard, and E. Guyon, "Critical currents and pinning effect in superconducting alloy films spatially modulated in concentration," Sol. State Comm., vol. 11, pp. 1679-1682, 1972; H. Raffy and E. Guyon, "Dependence of critical current and field of periodically modulated superconducting alloys on modulation amplitude," Physica, vol. 108B, pp. 947-948, 1981.
[13] G. Stejic *et al.*, "Effect of geometry on the critical currents of thin films," Phys. Rev. B, vol. 49, pp. 1274-1288, 1994.
[14] M. Tachiki and S. Takahashi, "Anisotropy of critical current in layered oxide superconductors," Sol. State Comm., vol. 72, pp. 1083-1086, 1989.
[15] A. I. Larkin and Yu. N. Ovchinnikov, "Flux pinning in type II superconductors," J. Low Temp. Phys., vol. 34, pp. 409-428, 1979.
[16] R. Labusch, "Calculation of the critical field gradient in type II superconductors," Cryst. Lattice Defects, vol. 1, pp. 1-16, 1969.
[17] M. Tachiki, S. Takahashi, and K. Sunaga, "Driving and pinning forces acting on vortices in layered superconductors," Phys. Rev. B., vol. 47, pp. 6095-6105, 1993.
[18] E. H. Brandt, "Elastic and plastic properties of the flux-line lattice in type-II superconductors," Phys. Rev. B, vol. 34, pp. 6514-6517, 1986.
[19] A. Sudbø and E. H. Brandt, "Flux-line tilt moduli in anisotropic superconductors," Phys. Rev. Lett., vol. 66, pp. 1781-1784, 1991.